

# Hierarchical Attention-based Age Estimation and Bias Analysis

Shakediel Hiba, Yosi Keller\*

**Abstract**—In this work, we present a Deep Learning approach to estimate age from facial images. First, we introduce a novel attention-based approach to image augmentation-aggregation, which allows multiple image augmentations to be adaptively aggregated using a Transformer-Encoder. A hierarchical probabilistic regression model is then proposed that combines discrete probabilistic age estimates with an ensemble of regressors. Each regressor is adapted and trained to refine the probability estimate over a given age range. We show that our age estimation scheme outperforms current schemes and provides a new state-of-the-art age estimation accuracy when applied to the MORPH II and CACD datasets. We also present an analysis of the biases in the results of the state-of-the-art age estimates.

## I. INTRODUCTION

Humans regularly use facial images to determine their age. There has been significant research into accurate age estimation in computer vision and biometrics, for a variety of applications such as e-commerce [1], face recognition [2], and the retrieval of age-based data, to name just a few. Accurate age estimation entails multiple computational challenges, which are uncommon for face detection or recognition. Variations of face appearance due to aging are unknown, complex and may be affected by multiple intrinsic and extrinsic factors, such as ethnicity, gender, and lifestyle. Aging results in gradual changes in appearance, making close ages appear similar, but notable age differences alter appearance significantly [3].

It is common to formulate estimating age based on face images as a classification problem, where an age  $a$  of the face  $x$  is classified as one of  $\{a_c\}_1^C$  discrete values [4], [5], [6], [7], [8], [9], or as the regression of  $a \in \mathbb{R}^+$ , given a high-dimensional embedding  $\hat{x}$  of the face  $x$  [5], [9], [4], [10], [11], [12]. The common approach to face-based biometric analysis is to first align the face image with a canonical spatial frame [13], and to analyze the cropped region of interest. Early approaches utilized local image descriptors [8] to encode the face images in high-dimensional representations used for regression by Kernel PLS [5]. The successful use of Deep Learning-based approaches in a variety of computer vision tasks paved the way for the development of end-to-end trainable age estimation schemes [14], [15] using classification or regression losses. Metric learning was used in both shallow [16] and CNN-based [14], [17], [18] schemes, where local features were learned using their age difference as a metric measure. Ranking-based approaches [19], [20], [21], [22] apply ordinal classification to utilize the ordinal structure of age labels to improve accuracy.

In this work, we present a CNN-based approach to improve age estimation using face images, which is depicted

in Fig. 1. Our *core contribution* is a novel attention-based aggregation of CNN embeddings of multiple augmentations of each input image. The aggregation (Fig. 1b) is applied in each training/test iteration, allowing the proposed network to adaptively weigh the optimal augmentations and improve the robustness to appearance and geometrical variations. This approach follows encoder-based schemes [23], where a sequence of word embeddings is aggregated in a *single* embedding vector by a Transformer-Encoder [24]. In contrast, the common approach is to utilize a *single* augmentation in each training/test iteration, where multiple augmentations are aggregated over multiple training iterations, or by using Test Time Augmentation (TTA) [25] depicted in Fig. 1a. Thus, our approach is applied to the embedding vectors and not to the spatial domain of each embedding (activation map). The aggregation approach can be applied to *any* network that provides an activation map, and is detailed and experimentally evaluated in the context of age estimation. We also present a hierarchical probabilistic regression scheme that learns an ensemble of age regressors, each relating to a limited age range, respectively, and the probability of each age range. Thus, we leverage the robustness of CNN-based probability estimation, with the precision of age regressors of limited age domains. Our approach is shown to outperform previous work that used classification [4], [12], ordinal classification [19], [20], [21], [26], tree-like structures [27], and deep hierarchies [27].

Bias analysis is a fundamental issue in biometrics in this day and age that was studied in the context of face recognition [28], [29], [30], [31] and age estimation [32], [33], [34]. We present a bias analysis of the proposed age estimation scheme, with respect to ethnicity and gender. Ours is the first bias analysis in face-based age estimation using a scheme achieving state-of-the-art (SOTA) accuracy (MAE $\approx$ 2.5 years).

In particular, we propose the following contributions:

- To improve face image embedding, we propose a novel transformer-based augmentation and embedding aggregation approach.
- We derive a hierarchical probabilistic age estimation scheme where the probabilistic age estimate allows us to optimally weigh the results of an ensemble of local age regressors.
- The proposed scheme is shown to achieve a new SOTA precision when applied to the MORPH II [35] and CACD [36] age estimation datasets.
- The estimation bias of our scheme is analyzed with respect to gender and ethnicity.

S. Hiba and Y. Keller are with the Faculty of Engineering, Bar Ilan University, Ramat-Gan, Israel. Email: yosi.keller@gmail.com

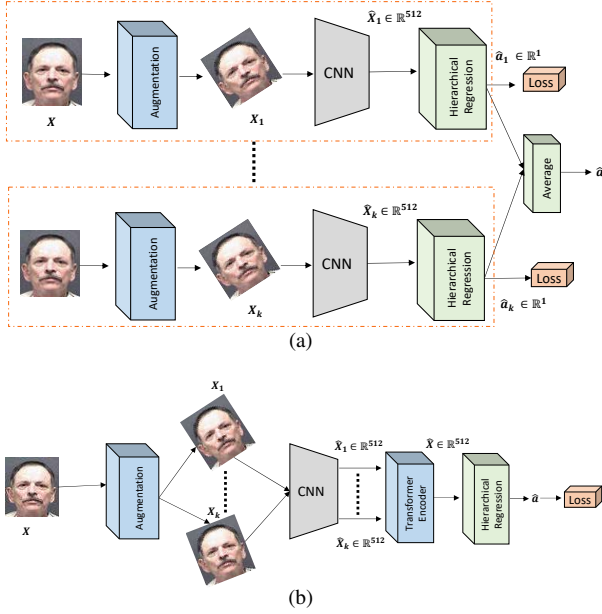


Fig. 1: The proposed attention-based augmentation aggregation vs. Test Time Augmentation (TTA) [25]. (a) In TTA, a network is trained using a *single* augmentation of the input  $x$ . In *run-time* the input is augmented  $\mathbf{K} = 10$  times, the network is run  $K$  times *separately*, and the results are averaged. (b) We propose using a *single network* to create  $K = 10$  different augmentations  $\{x_i\}_1^K$  from each input  $x$ , embed them through a CNN backbone  $\{\hat{x}_i\}_1^K$ , and aggregate the sequence of embeddings using the Transformer-Encoder. The aggregated feature vector  $\hat{x}$  is fed into the hierarchical regression. In *run-time* the same network is run *once*.

## II. RELATED WORK

The estimation of age from a face image is challenging due to differences between ethnicities, genders, and lifestyles in facial aging characteristics [37]. In their seminal work, Buolamwini and Gebre [29] demonstrated the importance of ethnicity and gender in face analysis and recognition, and this topic is of particular interest today.

Guo and Mu [9] proposed a two-step procedure, which classifies gender and ethnicity first, and then estimates age separately for each sub group. The shallow approaches used local image features to embed faces, followed by statistical inference. Thus, Balmaseda *et al.* [8] used Local Binary Pattern (LBP) features and SVM classifiers to compute multiscale normalized face images, alongside their local context. Zheng and Sun [7] used a ranking SVM, where age is estimated by first learning ranking relationships, which were used alongside the reference set to estimate age. Eidingger *et al.* [4] proposed a gender and age classification scheme for images of non-frontal faces acquired under uncontrolled conditions. Regression-based approaches formulate the age estimation problem as a scalar regression given a high-dimensional image embedding. Chen and Gong [11] introduced a cumulative attribute for learning a regression model when only sparse and unbalanced data are available to estimate age and crowd density. Low-level

visual features extracted from sparse and unbalanced image samples are mapped onto a cumulative attribute space, where each dimension is related to a semantic interpretation.

CNN-based schemes forgo the use of handcrafted image descriptors, in favor of learnt image embeddings. Thus, Wang and Kambhampettu [10] proposed a hierarchical unsupervised neural network architecture to learn low-level translation-invariant features, used as inputs to a set of Recursive Neural Networks (RNNs). Manifold learning was applied to capture the underlying face aging manifold by projecting the feature vector into a low-dimensional, better discriminative subspace. Hassner and Levi [12] reported significant accuracy improvements by formulating the age estimation as a classification problem, and applying CNNs. Sendik *et al.* [15] applied deep metric learning to face features computed by a CNN, while a Support Vector Regressor (SVR) was applied to estimate age. Deep metric learning was also used by Liu *et al.* [14], who proposed a hard quadruplet mining scheme to improve the resulting embedding, while a regression-based loss was applied to estimate the age. Rothe *et al.* [38] derived a classification scheme in which the class probability distribution of the Softmax function was used to compute the empirical expectancy of estimated age. Pan *et al.* [39] proposed a multitask approach, first computing the empirical estimation probability of each age using the Softmax activation function. The  $L_2$  loss, as well as the empirical variance of the age estimation error, were minimized. Malli *et al.* [40] suggested an ensemble of CNN-based classification models, where each ensemble model was trained to classify within a different age domain. The final inference was computed by averaging over the models' outputs. Tree-based approaches were also proposed [27], [41].

Shen *et al.* [41] propose a novel methodology that integrates Regression Forests with deep learning techniques. In this hybrid framework, the nodes of the Regression Forest are engineered to adaptively partition the input data. These nodes are then linked to fully connected layers within a Convolutional Neural Network (CNN). The optimization of both the Random Forests and the CNN is carried out simultaneously through an end-to-end training process. Li *et al.* [27] used a tree-based structure in which adjacent tree leaves in nearby branches were jointly connected to create a continuous transition, as well as an ensemble of local regressors. Each leaf is connected to a particular local regressor. The ordinality of the estimated ages was utilized by encoding the age labels in an ordinality-preserving representation [19], [20], [21], [26], where each model output determines whether an estimated age is higher than a given threshold. Such approaches have been shown to improve the accuracy of age classification. Niu *et al.* [20] used an ordinal regression CNN to resolve non-stationarity in aging patterns and developed the Asian Face Age Dataset (AFAD) which contains more than 160K images with precise age ground-truths labels. The Deep Cross-Population (DCP) domain adaptation approach to age estimation was proposed by Li *et al.* [17]. A CNN is trained using a large training dataset to improve the accuracy of the age estimation on a smaller test dataset. With DCP, transferable aging features are first learned using the source dataset and then transferred to the

target dataset. The aging features of the two populations are then aligned using an order-preserving pair-wise loss function. A correlation learning method for representing and exploiting inter/intra-cumulative attribute relationships is proposed in Tian et al. [18]. Utilizing correlations between and within gender groups, the approach is further extended to perform gender-aware age estimations.

Multiple image datasets have been used in face-based age estimation. Some legacy datasets such as the FG-NET [42] (1K images), FERET [43] (14K images), Chalearn LAP 2015 [44] (7.5K images) and UTKFace [45] (16K images) are too small for CNN-based schemes, while others such as the IMDB-Wiki [38] are based on web-scraping without an objective ground truth age estimate, using human annotators. As the accuracy of computational age estimation schemes improves ( $MAE \approx 2.5$  years), their accuracy is on par with the human annotations, limiting their effectiveness in future works. The MORPH Album II [35] (60K images) is of particular importance, as it provides accurate age labels. A particular downside of many of the datasets, such as the AFAD [20] and others, is that they do not provide identity labels. This restricted some works to only using the Random-Split (RS) test protocol, where the image set is *randomly* split into train and subsets. As in most datasets there are 5-25 images of each subject, this inevitably leads to *significant train-to-test leakage*, making the age estimation results in these works less indicative. We focus on datasets with identity labels, allowing us to apply the Subject-Exclusive (SE) protocol, where *all* of the images of a particular subject are used in train *or* test, *but not in both*.

#### A. Attention and Transformers

The Attention mechanism [46] is a class of contemporary neural network layers that aggregate information within input sequences. The inputs are aggregated by computing aggregation (attention) weights using the inner products between the input sequences. Attention layers are often stacked to improve inference capacity, and were applied to both sequence-to-sequence (NLP translation) and sequence-to-one (sentiment analysis) problems. In self-attention, attention weights are calculated with respect to a *single* input series, and the module is denoted as an *Encoder*. By computing the inner products between the (single) input sequence and itself, the encoder maps the input sequence into a higher dimensional space. The inputs to a *Decoder* are the key and query sequences used to compute the attention weights, to aggregate the value sequence. Attention models allow to computationally emphasize the contribution of the task-informative image cues, in contrast to the visual clutter present in most images. Transformers were introduced by Vaswani et al. [24] as a novel formulation of attention-based stacked layers, allowing encoding sequences without RNN layers such as LSTM and GRU. Transformer-based encoders and decoders utilize multiple stacked Multi-Head Attention (MHA) and Feed Forward layers. In contrast to the sequentially structured RNNs, the relative position and sequential order of the sequence elements are induced by positional encodings that are added to the Attention embeddings. Transformers were shown to provide

a computationally efficient framework for most NLP tasks [23], achieving SOTA performance, and were also applied in a variety of computer vision tasks [47]. In this work, we were inspired by recent attention-based single-sentence classification tasks in NLP [23], such as sentiment analysis. The gist of such approaches is to aggregate and encode an ordered sequence of word embeddings in a *single* embedding used for inference. Multiple such NLP tasks [23] use the same sequence (sentence) Transformer-Encoder-based aggregation, and differ on the dataset and training loss per task. In our approach, the sequence of augmented image embeddings is unordered. Thus, there is no need for positional encoding.

#### B. Bias Analysis

The significant accuracy improvement of face-based biometrics, such as face recognition, gender and ethnicity identification and age estimation, has resulted in a proliferation in their deployment in a gamut of applications. In particular, face-based biometrics were used by law enforcement agencies and commercial vendors. In their seminal work, Buolamwini and Gebru [29] showed the inherent bias of contemporary SOTA face recognition systems with respect to gender and ethnicity. Similarly, Wang et al. [48] studied ethnicity bias for multiple SOTA commercial and academic face recognition schemes. For that, they proposed the Racial Faces in the Wild (RFW) database, for which the ethnicity of each subject was thoroughly validated. They also propose a domain adaptation scheme to reduce ethnicity bias in face recognition.

Robinson et al. [31] introduced the novel Balanced Faces In the Wild (BFW) dataset, which is gender and ethnicity-balanced, to study the bias in state-of-the-art facial recognition systems. Different thresholds are shown to be required for recognition across different subgroups, and there is a significant improvement in performance. Human evaluations show that human perception exhibits similar biases. In a subsequent study, Robinson et al. [34] proposed a novel domain adaptation learning scheme for facial embeddings computed using CNNs, to mitigate unbalanced performance between ethnicity and gender subgroups, thus improving accuracy. The facial embeddings generated maintain identity while reducing demographic information to enhance privacy and reduce bias.

The accuracy bias of face recognition due to ethnicity or skin tone was also studied by Krishnapriya et al. [49] who showed that for a fixed decision threshold, Caucasian face images have a higher false non-matching rate, while the face images of African-Americans are characterized by a higher false matching rate. In particular, one-to-many identification might have a low false-negative identification rate, while having significant false-positive identification rates. Drozdowski et al. [30] presented a detailed survey of recent results in biometric algorithmic bias. The bias in subjective age estimation by human observers was studied by Clapes et al. [33]. The bias is shown to be related to attributes of the face images, such as gender, ethnicity, makeup, and expression. Additionally, they demonstrated that using apparent age labels rather than real ages improves the accuracy of CNN-based age estimation. The joint classification of gender, age, and race was studied

by Das et al. [32], using a multitask CNN (MTCNN), as well as the mitigation of biometric bias on the UTKFace and Bias Estimation in Face Analytics (BEFA) datasets. Puc et al. [50] found that face-based age estimation is consistently more accurate for men than for women, whereas ethnicity does not appear to have a significant or consistent effect. Their analysis was carried out using non-SOTA approaches, such as  $MAE \approx 7$ , compared to  $MAE \approx 2.5$  in contemporary schemes [35]. Hence, to the best of our knowledge, our work is the first to report SOTA age estimation with a bias analysis.

### III. HIERARCHICAL ATTENTION-BASED AGE ESTIMATION

In this work, we propose a deep learning-based scheme to estimate a subject’s age  $\hat{a}$  given the face image  $x$ . An overview of the proposed scheme is shown in Fig. 1. It consists of a novel self-attention embedding (SAE) architecture based on a Transformer-Encoder, and a hierarchical regression framework. In the image embedding phase, detailed in Section III-A, given an input image  $x$ , we create  $K$  corresponding augmentations  $\{x_i\}_1^K$ , and compute their embeddings  $\{\hat{x}_i\}_1^K$  using a backbone CNN. The embeddings  $\{\hat{x}_i\}_1^K$  are aggregated by a Transformer-Encoder, resulting in a fused embedding vector  $\hat{x}$ . The fused embedding is processed by a hierarchical regression that estimates age probabilities, and a corresponding ensemble of age regressors, such that the regressors’ output is adaptively weighted by the classification probabilities, as detailed in Section III-B.

#### A. Self-Attention-based Image Embedding

We propose a novel augmentation and self-attention-based embedding (SAE) to compute an image embedding that is robust to appearance variations, as shown in Fig. 1. For that, each input image  $x$  is augmented  $K$  times to create the set of augmented images  $\{x_i\}_1^K \in \mathbb{R}^{224 \times 224}$ . The image augmentations used follow previous work and are detailed in Section IV-B. We also experimented in learning the augmentations using RandAugment [51], but this did not improve the accuracy. Each of these image augmentations  $x_k \in \{x_k\}_1^K$  is embedded using a CNN backbone. Any CNN can be used, and we evaluated multiple backbones, as detailed in Section IV, to compare with the contemporary schemes in which they were used. The set of embeddings  $\{\hat{x}_i\}_1^K \in \mathbb{R}^{512}$  is aggregated into a single embedding vector  $\hat{x}$  using a Transformer-Encoder. As the sequence of augmentation embeddings are unordered, there is no need for positional encoding, and the encoding is derived by adding a fully learnt *class token*  $\in \mathbb{R}^{512}$  to the encoded series. The aggregated representation  $\hat{x}$  is the Transformer-Encoder’s output corresponding to the cls token. Our attention-based augmentation-aggregation method improves image embedding for age estimation, as demonstrated in Section IV-A through Tables IV and IV

#### B. Hierarchical probabilistic age regression

The inference phase in deep learning-based age estimation schemes is based on classification [12] and regression [19], [20], [21], [26]. Classification-based schemes aim to classify

the estimated age  $a$  of a face image into one of  $\{a_c\}_1^C$  ages. The accuracy of regression schemes can be improved by using an ensemble of regressors  $\{R_c(\hat{x})\}_1^C$  [27], [41], where each regressor  $R_c(\hat{x})$  estimates the residual regression with respect to the discrete label  $a_c$ . We propose to utilize the upside of both classification and regression approaches using the framework shown in Fig. 2, where instead of classifying the age  $\hat{a} \in \{a_c\}_1^C$  we estimate the age probabilities  $P(a = a_c)$  that are used to estimate the age expectancy

$$\hat{a} = \sum_c P(a = a_c) R_c(\hat{x}). \quad (1)$$

The classifier is optimized by multiple losses: the first is the cross-entropy loss  $L_{CE}$  that optimizes the classification probability  $P(a = a_c)$ . The second is the Mean-Variance Loss [39] consisting of the following two terms:

$$L_M = \frac{1}{2N} \sum_{i=1}^N \left( \sum_{c=1}^C P(a = a_c) \cdot c - a_i^0 \right)^2 \quad (2)$$

$$L_V = \frac{1}{N} \sum_{i=1}^N \sum_{c=1}^C P(a = a_c) \left( c - \sum_{c=1}^C c \cdot P(a = a_c) \right)^2, \quad (3)$$

where  $N$  is the number of points in a batch. Equation 2 minimizes the mean square error (MSE) between the empirical expectation and the ground truth  $a_i$ , while Eq. 3 minimizes the empirical variance of the estimate. The regression ensemble  $\{R_c(\hat{x})\}_1^C$  is optimized by a corresponding set of  $L_2$  losses  $\{L_{MSE}^c\}_1^C$ , where  $L_{MSE}^c$  is the Mean Square Error loss applied to  $\hat{a}_c$ , the result of regressor  $c$ . The overall loss is thus given by

$$L = \lambda_1 L_{CE} + \lambda_2 L_M + \lambda_3 L_V + \lambda_4 \sum_c L_{MSE}^c, \quad (4)$$

where  $\{\lambda_i\}_1^4$  are predefined weights (Section IV-B).

Our work, assumes that the face aging process is episodic, implying that although aging is a continuous process, faces from close ages are more visually similar than others farther away, and that this process differs notably at different ages. Hence, the age in each age episode  $c$  is estimated by a particular regressor  $R_c(\hat{x})$ . Despite the episodic nature of aging, it is continuous, so restricting each local regressor  $R_c(\hat{x})$  may cause significant marginal effects. Thus, we formulate the final estimation as in Eq. 1 to allows joint optimization and end-to-end training of both the probability estimator and the ensemble of regressors  $\{R_c(\hat{x})\}_1^C$ . Due to the ordinal classification and the mean-variance loss, far-away local estimates are less likely to receive a high probability, such that local estimators will receive less significance the farther away they are from the expected age. In case of misclassification to neighboring classes, the nearby local estimators can compensate and provide a robust estimate.

## IV. EXPERIMENTAL RESULTS

### A. Datasets

MORPH Album II [35] is one of the largest longitudinal face databases available. It contains 55,134 facial images of

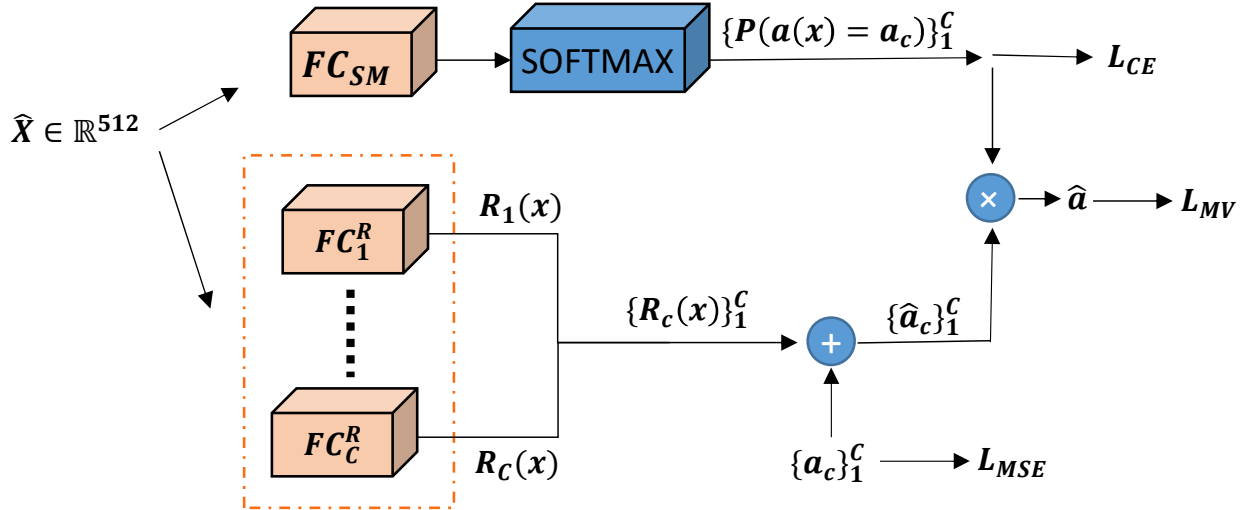


Fig. 2: The proposed hierarchical regression framework. The input feature vector  $\hat{x}$  is jointly processed by two parallel branches: the upper is the classifier and probability estimator, while the lower is the regression ensemble  $\{R_c(\hat{x})\}_1^C$ . The age estimate  $\hat{a}$  is given by the empirical expectancy of  $\{\hat{a}_i\}_1^C$ . The upper classification subnetwork is optimized by the Cross-Entropy loss  $L_{CE}$ . The outputs of the ensemble of local regressors are optimized by the Mean Square Error loss  $L_{MSE}$ . The network’s age estimate  $\hat{a}$  is optimized by the Mean-Variance Loss [39]  $L_{MV}$ .

13,617 subjects with ages 16-77, such that each subject is depicted in multiple images, the identity of the subject in each image is known. All images are mugshots taken in a controlled environment of good image quality, centered faces poses, and neutral faces expressions. The dataset depicts both genders, and multiple ethnic groups, mostly white and black. Its demographic and gender breakdown is reported in Table I. The CACD dataset [36] contains 163,446 images of 2,000 celebrities between the ages of 14 and 62, collected from the Internet. The identity of the subject in each image is given.

We follow two evaluation protocols used in previous works [39], [21] to define the training and testing sets, The first, is the Random-Split (RS) protocol, in which the face images are randomly split to train and test sets, such that the images of the *same* person might appear in *both* train and test sets. This creates a leakage between the train and test sets, as it essentially mixes age estimation with age recognition. Thus, a face recognition scheme, without age estimation training, can achieve perfect age estimation accuracy. The second protocol is the Subject-Exclusive (SE) protocol, where identities are randomly split to be either train or test, but not both, to avoid leakage. Due to leakage, the RS accuracy is significantly higher than the SE scores for *all* schemes and datasets. Hence, we submit that the RS metric should be considered less reliable and avoided in future work when possible. In this work, we report the RS results due to legacy results that we compare to. The MORPH II and CACD datasets can be used to assess the accuracy of age estimation using both protocols.

We avoided using the small-scale datasets that are too small for our Transformer-driven approach: FG-NET [42], FERET [43], Chalearn LAP 2015 [44] and UTKFace [45]. We also avoided the AFAD dataset [20] that is missing the identities, implying that only the RS protocol can be applied.

TABLE I: The demographic breakdown of the Morph II dataset [35].

	Black	White	Asian	Hispanic	Other
<b>Male</b>	36,832	7,961	141	1,667	44
<b>Female</b>	5,757	2,598	13	102	19
<b>Total</b>	42,589	10,559	154	1,769	63

### B. Implementation Details

The age estimation accuracy is evaluated by the standard Mean Absolute Error (MAE) that was used in all previous works. MAE is calculated using the mean absolute error between the predicted age  $\hat{a}_i$  and the ground truth  $a_i$

$$MAE = \frac{1}{N} \sum_i |\hat{a}_i - a_i|, \quad (5)$$

where  $N$  is the number of test images. The lower the MAE the better the accuracy. We used the CNN Vgg-16 [52] and ResNet-34 [53] CNN backbones that were used in previous SOTA age estimation schemes, so that the comparison could be based only on the proposed architecture rather than the backbone. The proposed age estimation scheme is trained in two phases. First, we adapt the CNN Vgg-16 [52] and ResNet-34 [53] ImageNet-based backbones to face recognition using the MORPH II [35] training set and Arcface loss [54]. We then train the entire proposed solution end-to-end. The input face images were first detected, cropped, and aligned by the RetinaFace detector [13] and then resized to a size of  $224 \times 224$ . The proposed attention-based aggregation was implemented using a Transformer-Encoder with four blocks, a dropout of  $p = 0.1$ , where each block contains an MHA layer with four

heads. Each input image was augmented to  $K = 10$  images, such that multiple augmentations were randomly applied with a probability of 0.5: horizontal flips, color jittering, random affine transformation and randomly erasing small parts of the image [55]. We also applied the RandAugment [51] approach, but did not improve accuracy. The classifier in Section III-B and the corresponding ensemble of classifiers  $\{R_c(\hat{x})\}_1^C$  were applied with  $\{a_c\}_1^C = \{1, 2, \dots, 75\}$ . We used the Ranger optimizer, a combination of Rectified Adam [56] with the Lookahead technique [57], and a Cosine Annealing learning rate decay [58]. All experiments were carried out using a single NVIDIA GTX 1080 TI and the PyTorch framework. Loss hyperparameters  $\lambda_i$  in Eq. 4 are set to: 0.2, 0.05, 1, 1 accordingly, where the parameters  $\lambda_1, \lambda_2, \lambda_3$  were taken from [39], and  $\lambda_4=1$  is in accordance with  $\lambda_3$ .

### C. Results

We compare our approach with multiple SOTA methods using the MORPH II [35] and CACD [36] datasets, and the results are reported in Tables II and III, respectively. The results of previous schemes are quoted from their respective publications that used the same protocol specifications as ours. Following previous works, we randomly split the datasets to 80% train and 20% test in both the RS and SE protocols. Table II shows that our approach outperforms all previous methods in the MORPH II data set using the RS and SE protocols. The RS accuracy (MAE = 1.13) is significantly higher than the SE accuracy (MAE = 2.53). We attribute that, as before, to leakage in the RS protocol, making the RS results less indicative.

TABLE II: Age estimation results evaluated using the **Morph-II dataset II**. We compare with previous SOTA schemes using both the RS and SE protocols.

Method	Backbone	MAE	Protocol
Human [37]		6.30	
Oh-rank[6]	AAM	6.07	RS
Ranking-CNN[19]	ALEXNET	2.96	RS
OR-CNN[20]	proprietary	3.27	RS
M-lsdml[14]	RESNET101	2.89	RS
Coral[26]	RESNET34	2.64	RS
Dex[38]	VGG16	3.25	RS
Dex(pretrained)[38]	VGG16	2.68	RS
M-lsdml[14]	VGG16	2.91	RS
Mean-Variance[39]	VGG16	2.16	RS
BridgeNet[27]	VGG16	2.63	RS
DCDL[59]	VGG-16-BN	2.45	RS
Knowledge Distil[22]	proprietary	1.95	RS
<b>ours</b>	VGG16	<b>1.13</b>	RS
Coral[26]	RESNET34	3.27	SE
Mean-Variance[39]	VGG16	2.79	SE
soft-ranking[21]	RESNET34	2.83	SE
soft-ranking[21]	VGG16	2.71	SE
DCDL[59]	VGG-16-BN	2.62	SE
<b>ours</b>	VGG16	<b>2.53</b>	SE

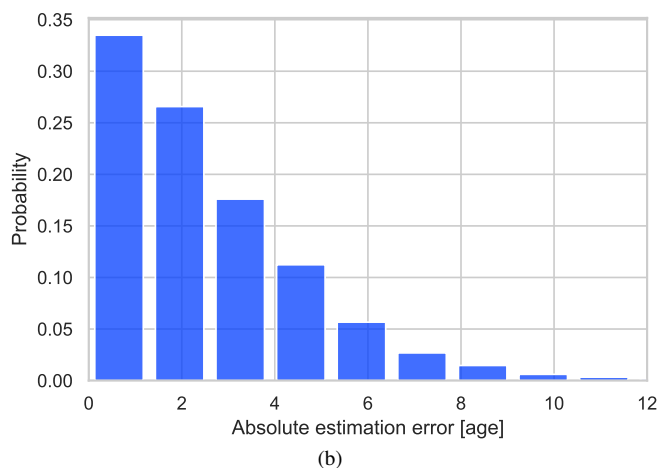
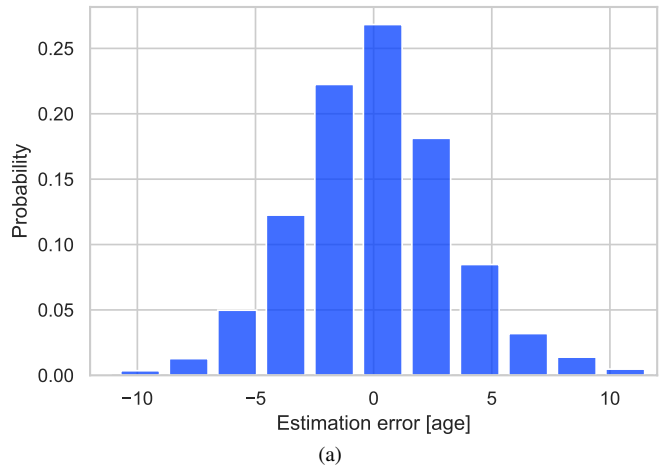


Fig. 3: The distribution of the age estimation errors. The proposed scheme was applied to the Morph II dataset.

The distribution of the age estimation errors shown in Fig. 3 resembles a Gaussian distribution centered around zero, where most estimation errors ( $\approx 77\%$ ) are within an interval of three years. In particular, our hierarchical probabilistic approach outperforms Li et al. [27], that also divide the age axis into multiple overlapping subdomains and employ local regressors over those subdomains, while using the same backbone as ours. We also outperform the Mean-Variance approach [39] that employs the same backbone and losses.

In Table III, we report the results for the CACD dataset. We used the RS protocol and compared it with the previous SOTA results of Cao et al. [26] and Li et al. [60]. Our scheme outperformed the other schemes, although we used a shallower backbone (VGG16) compared to the Inception-v3 [26] and RESNET50 [60]. In particular, an accuracy gain of 0.9% was achieved compared to using the same VGG16 backbone in [26]. We also applied the SE protocol. We are the first, to the best of our knowledge, to evaluate it over this dataset. We compare the variants of the proposed scheme, with and without the proposed Transformer-Encoder augmentation aggregation. The encoder improves accuracy by  $\approx 0.5\%$ . As in Table II, the RS errors are lower by  $\approx 1\%$ , implying there exists a

TABLE III: Age estimation results evaluated using the **CACD dataset** [36]. We compare with previous SOTA schemes [26], [60] using the RS protocol. We also applied the SE protocol with and without the proposed Transformer-Encoder-based augmentation aggregation.

Method	Backbone	MAE	Protocol
Coral[26]	RESNET34	5.25	RS
Coral[26]	Inception-v3	4.90	RS
RNDF[60]	RESNET50	4.60	RS
<b>ours</b>	VGG16	<b>4.32</b>	RS
ours(CNN)	VGG16	5.80	SE
<b>ours</b>	VGG16	<b>5.35</b>	SE

significant leakage between the random training and test sets.

#### D. Ablation study

To evaluate the contribution of each of the proposed algorithmic components, we performed multiple ablation studies. In each ablation experiment, we modified a single algorithmic component or hyperparameter to evaluate it, and applied the resulting implementation to the MORPH II dataset that allows us to apply both the RS and SE protocols. The baseline scheme is derived from Table II.

TABLE IV: Ablation study of the proposed attention-based augmentation-aggregation scheme. We compare the performance of our proposed architecture with a different number of augmentations at input ( $K$ ). ‘1 no-encoder’ refers to using a single augmentation without an encoder. ‘10 average-pool’ refers to using 10 augmentations that are aggregated by averaging the activations maps.

#Augs	MAE
1 no-encoder	2.63
2	2.60
4	2.58
6	2.54
<b>10</b>	<b>2.53</b>
10 average-pool	2.58
15	2.60

We first evaluated the SAE attention-based augmentation-aggregation scheme, detailed in Section III-A, using the face images. For that we implemented two additional variations: the first (1 no-encoder), is a naive baseline without augmentations and aggregations, where we only uses a single replica of the input image. This results in the lowest accuracy of 2.63. When 10 augmentations were applied using average pooling (10 average-pool), the accuracy improved to 2.58 compared to our SOTA of 2.53. Regarding the number of augmentations used, the results shown in Table IV exemplify the effectivity of the proposed augmentation-aggregation. In particular, using additional augmentations per image improves the estimation

accuracy up to using 10 augmentations; applying additional augmentations did not improve the accuracy. We suggest that the proposed aggregation scheme is of general applicability and can be applied to any task where the input image can be augmented.

TABLE V: Ablation study of varying Transformer-Encoder parameters: the number of encoder layers and attention heads.

#layers	#heads	MAE
8	8	2.57
<b>4</b>	<b>4</b>	<b>2.53</b>
2	2	2.55

The encoder configuration was examined by trying out multiple configurations. The more encoder layers are used, the larger the network’s learning capacity. But this might also lead to overfitting. Indeed, the results in Table V show that the ‘sweet spot’ is achieved for four layers and four MHA. Using a deeper configuration leads to overfitting. We also verified the choice of the age classification bin size and corresponding classification ensemble  $\{R_c(\hat{x})\}_1^C$ . The highest precision is achieved for  $binsize = 1$ .

TABLE VI: Ablation study of the classification bin size and corresponding regression ensemble  $\{R_c(\hat{x})\}_1^C$ .

Binsize	MAE
10	2.56
5	2.56
<b>1</b>	<b>2.53</b>

#### E. Bias Analysis

Following the discussion in Section II-B, we present a statistical bias analysis based on the MORPH II dataset, whose gender and ethnicity breakdowns are given in Table I. The MORPH II dataset is imbalanced in terms of the age, gender, and ethnicity. Our approach, as well as all prior schemes, was trained by randomly sampling the dataset, resulting in an ethnically and gender-wise imbalanced and biased training and test sets. We report for the first time, to the best of our knowledge, bias estimates for a scheme that is of SOTA accuracy ( $MAE \approx 2.5$  years). In our bias analysis, we use the SE protocol and the proposed SOTA network, as in Table II.

**Age bias.** The error distribution vs. estimated age is reported in Table VII. Age estimation errors result from the given number of training samples per age range, as well as age-related appearance changes that are hard to quantify. The 15-25 age range has the lowest estimation error. As the number of training samples is relatively small, we attribute it to the accelerated rate of changes in physiological appearance, making the age estimation easier. The error flattens for the 30-50 age range, which contains most of the training samples, but increases for the 55-70 age range, where there are fewer samples.

TABLE VII: **Age bias.** The number of MORPH II samples per age category, and the corresponding MAE and standard deviation of the age estimation error in each category.

Age	#Samples	MAE	Std
15-20	3330	1.52	1.74
20-25	9703	2.00	1.65
25-30	8243	2.25	1.95
30-35	6243	2.96	1.99
35-40	8638	2.87	2.36
40-45	7552	2.69	1.95
45-50	5884	2.69	2.24
50-55	3421	3.28	2.47
55-60	1569	3.90	3.14
60-65	399	5.99	2.94
65-70	124	6.81	2.55

**Gender and ethnicity bias.** In biometrics, gender and ethnicity are the most common sources of estimation bias [31]. In Figure 4, we examine the ethnicity bias, that does not appear to be significant, although the MORPH II database is heavily skewed towards Black men, making up 67% of the dataset (Table I). Figure 5 presents the gender-specific estimation accuracy. The estimation error rate for men is lower by close to 10% due to the large number of male training samples. Figures 6 and 7 breakdown the bias and MAE due to gender and ethnicity, where the error for female subjects is greater for all ethnicities. It is substantially higher for black and female subjects, respectively, by nearly 0.8 and 0.5 years. However, it is biased towards female subjects by an average error of 0.7 years. The results are similar to those of Puc et al. [50] that used different schemes and evaluation datasets.

**Age estimation bias due to imbalanced training sets.** The demographics of the MORPH II [35] dataset, detailed in Table I, are significantly skewed in favor of men vs. women, 77% and 23%, respectively. We mitigated the gender imbalance to evaluate its influence. Hence, we followed Robinson et al. [34], [31] by creating a gender-balanced image set based on MORPH II dataset. We used all 8489 female images and randomly sampled the men identities until we attained the same number of men face images. The set was split 80% and 20% for the training and test tasks, respectively. We retrained the VGG16-based age estimation network using the gender-balanced training set using the SE protocol as in Section IV-C. The results are shown in Fig. 8, and we compare to Fig. 7 where the full MORPH II set was used. The estimation accuracy decreased similarly for black and white men by  $\sim 0.95$  years, while that of woman decreased by  $\sim 0.35$  years. This implies that the absolute accuracy of age estimation is mostly influenced by the number of training samples. Since the men estimation accuracy degraded, the bias in their favor decreased.

#### F. Self-Attention-based Embedding

In order to exemplify the general applicability of the Self-Attention-based Embedding (SAE) approach, introduced in

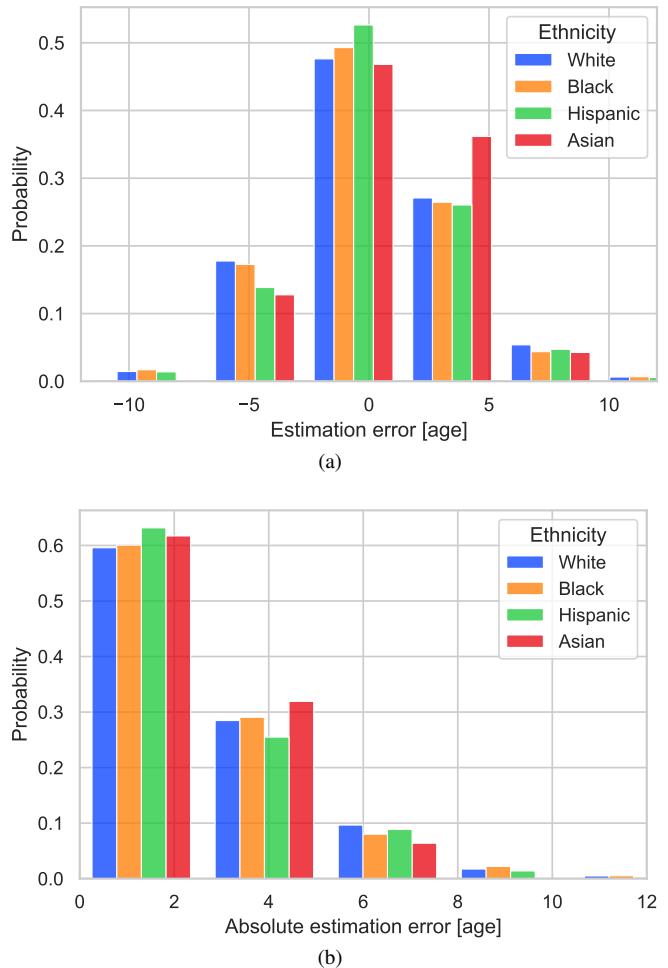


Fig. 4: **Ethnicity bias.** The MAE per ethnicity over the Morph II dataset. There is no apparent ethnicity-related estimation bias. We attribute the slight difference in the results of Asian woman to their number (13) in the dataset. Please consider the ethnicity/gender breakdown in Table I.

Section III-A, it was applied to the classification of the CIFAR-10 and CIFAR-100 datasets [61]. The CIFAR-10 dataset consists of 10 classes with 5000 training images and 1000 testing images per class, while the CIFAR-100 dataset has 100 classes with 500 training images and 100 testing images per class. The images in both datasets are  $32 \times 32$  pixels and have been previously used to evaluate learning schemes. We used the SAE approach with varying parameters to classify images using shallow and deep neural networks and observe their impact on the accuracy. The CIFAR-10 dataset was tested with a shallow<sup>1</sup> and the VGG16 networks, while the more challenging CIFAR-100 dataset was tested with the VGG16, RESNET18, RESNET34 and RESNET50 networks. We also compared to a SAE formulation based on Average Pooling, instead of a Transformer-Encoder. All networks were trained using a batch size of 64, an Adam optimizer with weight decay of  $1e-5$ , and an initial learning rate of  $1e-4$  during all

<sup>1</sup>[https://pytorch.org/tutorials/beginner/blitz/cifar10\\_tutorial.html?highlight=data%20loader](https://pytorch.org/tutorials/beginner/blitz/cifar10_tutorial.html?highlight=data%20loader)



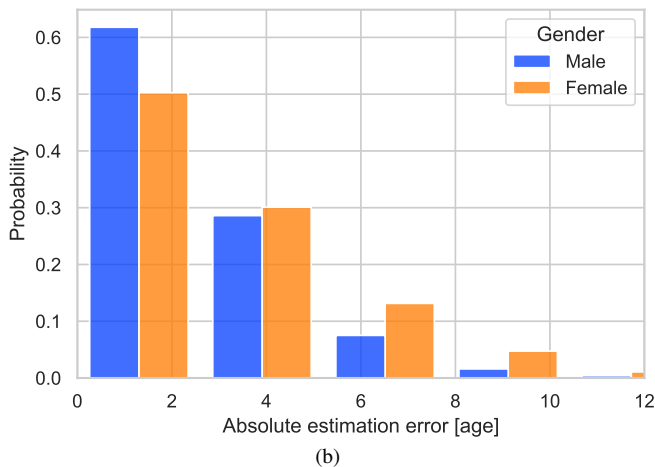
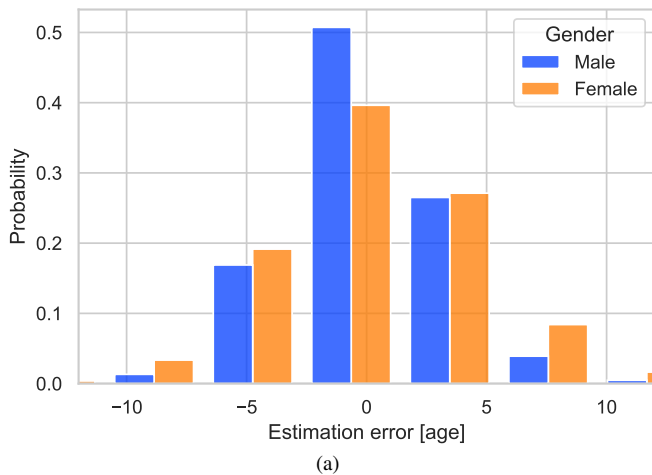


Fig. 5: **Gender bias.** Estimation MAE probability per gender over the Morph II dataset. The probability of low age estimation errors is higher by close to 10% for male images.

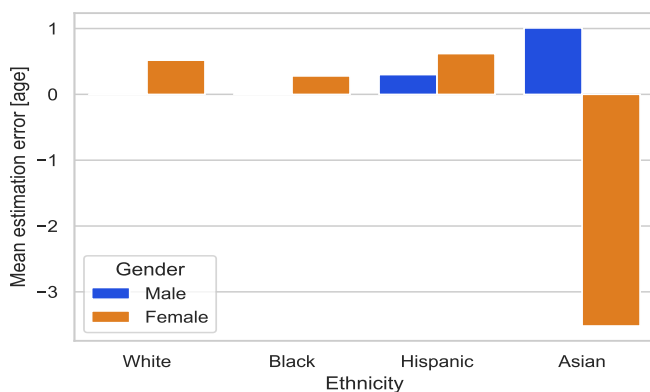


Fig. 6: **Gender and ethnicity bias.** The bias in age estimation per ethnicity and gender. The age bias for men is negligible.

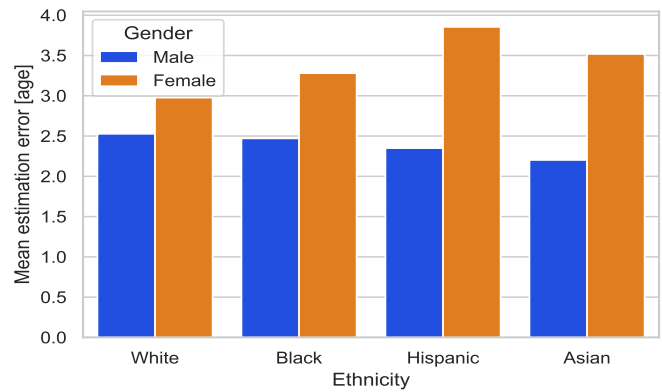


Fig. 7: **Gender and ethnicity MAE bias.** The MAE in age estimation per ethnicity and gender. The MAE for all men ethnicities is similar and for each ethnicity, it is smaller than that of the women.

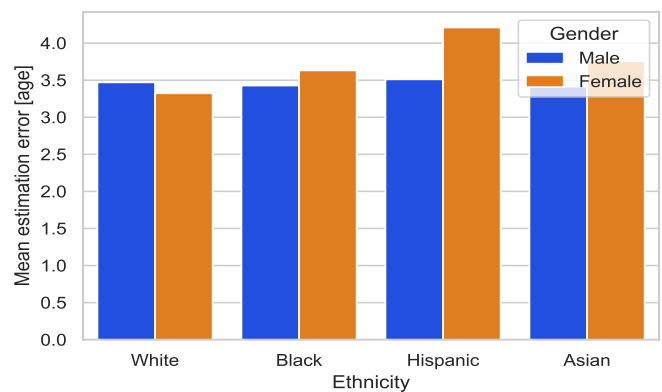


Fig. 8: **Gender and ethnicity MAE bias trained using the gender-balanced training set.** The MAE of the age estimation per ethnicity and gender. The network was trained using a gender-balanced training set based on the MORPH II dataset, reducing the age estimation bias compared to the estimates based on the gender-skewed MORPH II dataset in Fig. 7.

simulations. The learning rate was reduced by a factor of 0.2 if the loss did not decrease for more than 3 epochs. The self-attention was implemented using a single-layer Transformer-Encoder with two heads, which only required the addition of two fully connected layers. The classification accuracy results are shown in Table VIII and demonstrate that the SAE approach improves the accuracy of both shallow and deep networks, with the most significant improvement observed in the shallow CIFAR-10 network (from 56% to 68% accuracy). Using the Average-Pooling based SAE also improved the baseline results significantly, implying that using additional input image augmentations carried the heavy load in the SAE.

## V. CONCLUSIONS

In this paper, we present a novel approach for deep-learning age estimation from face images. First, we show that multiple augmentations can be encoded and aggregated by a Transformer-Encoder to yield a robust embedding. The

TABLE VIII: **Self-Attention-based Embedding.** The SAE was applied to the CIFAR-10 and CIFAR-100 datasets using different backbones. AvgPull refers to implementing the SAE using Average Pooling instead of a Transformer-Encoder.

Dataset	Backbone	#Aug	#layer	#heads	Acc. [%]
CIFAR-10	Shallow	1			56
CIFAR-10	Shallow	5		AvgPull	<b>72</b>
CIFAR-10	Shallow	3	1	2	62
CIFAR-10	Shallow	5	1	2	70
CIFAR-10	Shallow	5	2	2	<b>72</b>
CIFAR-10	Shallow	10	1	2	<b>72</b>
CIFAR-10	Shallow	15	1	2	<b>72</b>
CIFAR-10	VGG16	1			87
CIFAR-10	VGG16	5		AvgPull	90
CIFAR-10	VGG16	5	1	2	<b>90</b>
CIFAR-10	VGG16	5	2	2	<b>92</b>
CIFAR-10	VGG16	10	1	2	<b>90</b>
CIFAR-100	VGG16	1			60
CIFAR-100	VGG16	5	1	2	63
CIFAR-100	VGG16	10	1	2	<b>65</b>
CIFAR-100	RESNET18	1			59
CIFAR-100	RESNET18	5		AvgPull	64
CIFAR-100	RESNET18	5	1	2	<b>66</b>
CIFAR-100	RESNET18	10	1	2	<b>67</b>
CIFAR-100	RESNET34	1			61
CIFAR-100	RESNET34	5		AvgPull	66
CIFAR-100	RESNET34	5	1	2	<b>67</b>
CIFAR-100	RESNET34	5	2	2	<b>67</b>
CIFAR-100	RESNET34	10	1	2	<b>67</b>
CIFAR-100	RESNET50	1			58
CIFAR-100	RESNET50	5		AvgPull	65
CIFAR-100	RESNET50	5	1	2	<b>68</b>
CIFAR-100	RESNET50	10	1	2	<b>68</b>

second step is to propose a hierarchical probabilistic age estimation framework based on a deep classifier for estimating age probabilities. Probability estimates are used to weight a corresponding ensemble of local regressors, each adapted to a particular age subdomain. Our proposed scheme outperforms the current SOTA schemes. We also present, for the first time to our knowledge, a bias analysis of the SOTA results in face-based age estimation. We hope that the proposed bias analysis will be used by others in the field.

#### REFERENCES

- [1] A. Hakeem, H. Gupta, A. Kanaujia, T. E. Choe, K. Gunda, A. W. Scanlon, L. Yu, Z. Zhang, P. L. Venetianer, Z. Rasheed, and N. Haering, "Video analytics for business intelligence," in *Video Analytics for Business Intelligence*, 2012.
- [2] A. Lanitis, C. Draganova, and C. Christodoulou, "Comparing different classifiers for automatic age estimation," *IEEE Transactions on Systems, Man, and Cybernetics, Part B (Cybernetics)*, vol. 34, pp. 621–628, 2004.
- [3] V. Lambros, "Facial aging: A 54-year, three-dimensional population study," *Plastic and reconstructive surgery*, vol. 145, pp. 921–928, 04 2020.
- [4] E. Eiding, R. Enbar, and T. Hassner, "Age and gender estimation of unfiltered faces," *IEEE Transactions on Information Forensics and Security*, vol. 9, no. 12, pp. 2170–2179, 2014.
- [5] G. Guo and G. Mu, "Simultaneous dimensionality reduction and human age estimation via kernel partial least squares regression," in *Proceedings of the IEEE/CVF Conference on Computer Vision and Pattern Recognition (CVPR)*, June 2011, pp. 657–664.
- [6] K.-Y. Chang, C.-S. Chen, and Y.-P. Hung, "Ordinal hyperplanes ranker with cost sensitivities for age estimation," in *Proceedings of the IEEE/CVF Conference on Computer Vision and Pattern Recognition (CVPR)*, June 2011, pp. 585–592.
- [7] D. Cao, Z. Lei, Z. Zhang, J. Feng, and S. Z. Li, "Human age estimation using ranking svm," in *Biometric Recognition*, W.-S. Zheng, Z. Sun, Y. Wang, X. Chen, P. C. Yuen, and J. Lai, Eds. Berlin, Heidelberg: Springer Berlin Heidelberg, 2012, pp. 324–331.
- [8] E. Ramón-Balmaseda, J. Lorenzo-Navarro, and M. Castrillón-Santana, "Gender classification in large databases," in *Progress in Pattern Recognition, Image Analysis, Computer Vision, and Applications*. Springer, 2012, pp. 74–81.
- [9] G. Guo and G. Mu, "Human age estimation: What is the influence across race and gender?" in *IEEE Conference on Computer Vision and Pattern Recognition Workshops (CVPRW)*, June 2010, pp. 71–78.
- [10] X. Wang and C. Kambhampettu, "Age estimation via unsupervised neural networks," in *International Conference on Automatic Face and Gesture Recognition (FGA)*, vol. 1, May 2015, pp. 1–6.
- [11] K. Chen, S. Gong, T. Xiang, and C. Loy, "Cumulative attribute space for age and crowd density estimation," in *Proceedings of the IEEE/CVF Conference on Computer Vision and Pattern Recognition (CVPR)*, June 2013, pp. 2467–2474.
- [12] G. Levi and T. Hassner, "Age and gender classification using convolutional neural networks," in *IEEE Conference on Computer Vision and Pattern Recognition Workshops (CVPRW)*, June 2015, pp. 34–42.
- [13] J. Deng, J. Guo, E. Ververas, I. Kotsia, and S. Zafeiriou, "Retinaface: Single-shot multi-level face localisation in the wild," in *Proceedings of the IEEE/CVF Conference on Computer Vision and Pattern Recognition (CVPR)*. IEEE, 2020, pp. 5202–5211.
- [14] H. Liu, J. Lu, J. Feng, and J. Zhou, "Label-sensitive deep metric learning for facial age estimation," *IEEE Transactions on Information Forensics and Security*, vol. 13, no. 2, pp. 292–305, 2018.
- [15] O. Sendik and Y. Keller, "Deepage: Deep learning of face-based age estimation," *Signal Processing: Image Communication*, vol. 78, 08 2019.
- [16] R. Hadsell, S. Chopra, and Y. LeCun, "Dimensionality reduction by learning an invariant mapping," in *Proceedings of the IEEE/CVF Conference on Computer Vision and Pattern Recognition (CVPR)*, vol. 2, 2006, pp. 1735–1742.
- [17] K. Li, J. Xing, C. Su, W. Hu, Y. Zhang, and S. Maybank, "Deep cost-sensitive and order-preserving feature learning for cross-population age estimation," in *Proceedings of the IEEE/CVF Conference on Computer Vision and Pattern Recognition (CVPR)*, 2018, pp. 399–408.
- [18] Q. Tian, M. Cao, S. Chen, and H. Yin, "Relationships self-learning based gender-aware age estimation," *Neural Processing Letters*, vol. 50, no. 3, pp. 2141–2160, 2019.
- [19] S. Chen, C. Zhang, M. Dong, J. Le, and M. Rao, "Using ranking-cnn for age estimation," in *Proceedings of the IEEE/CVF Conference on Computer Vision and Pattern Recognition (CVPR)*, 2017, pp. 742–751.
- [20] Z. Niu, M. Zhou, L. Wang, X. Gao, and G. Hua, "Ordinal regression with multiple output cnn for age estimation," in *Proceedings of the IEEE/CVF Conference on Computer Vision and Pattern Recognition (CVPR)*, 2016, pp. 4920–4928.
- [21] X. Zeng, J. Huang, and C. Ding, "Soft-ranking label encoding for robust facial age estimation," *IEEE Access*, vol. 8, pp. 134 209–134 218, 2020.
- [22] Q. Zhao, J. Dong, H. Yu, and S. Chen, "Distilling ordinal relation and dark knowledge for facial age estimation," *IEEE Transactions on Neural Networks and Learning Systems*, vol. PP, 07 2020.
- [23] J. Devlin, M.-W. Chang, K. Lee, and K. Toutanova, "BERT: Pre-training of deep bidirectional transformers for language understanding," in *NAACL-HLT*. Minneapolis, Minnesota: Association for Computational Linguistics, Jun. 2019, pp. 4171–4186.
- [24] A. Vaswani, N. Shazeer, N. Parmar, J. Uszkoreit, L. Jones, A. N. Gomez, L. Kaiser, and I. Polosukhin, "Attention is all you need," in *Advances in Neural Information Processing Systems (NIPS)*, I. Guyon, U. von Luxburg, S. Bengio, H. M. Wallach, R. Fergus, S. V. N. Vishwanathan, and R. Garnett, Eds., 2017, pp. 5998–6008.
- [25] I. Kim, Y. Kim, and S. Kim, "Learning loss for test-time augmentation," in *Advances in Neural Information Processing Systems (NIPS)*. Curran Associates Inc., 2020.
- [26] W. Cao, V. Mirjalili, and S. Raschka, "Rank consistent ordinal regression for neural networks with application to age estimation," *Pattern Recognition Letters*, vol. 140, pp. 325–331, 2020.

- [27] W. Li, J. Lu, J. Feng, C. Xu, J. Zhou, and Q. Tian, "Bridgenet: A continuity-aware probabilistic network for age estimation," in *Proceedings of the IEEE/CVF Conference on Computer Vision and Pattern Recognition (CVPR)*, 2019, pp. 1145–1154.
- [28] J. G. Cavazos, P. J. Phillips, C. D. Castillo, and A. J. O'Toole, "Accuracy comparison across face recognition algorithms: Where are we on measuring race bias?" *IEEE Transactions on Biometrics, Behavior, and Identity Science*, vol. 3, no. 1, pp. 101–111, 2021.
- [29] J. Buolamwini and T. Gebru, "Gender shades: Intersectional accuracy disparities in commercial gender classification," in *Proceedings of the 1st Conference on Fairness, Accountability and Transparency*, S. A. Friedler and C. Wilson, Eds., vol. 81, 2018, pp. 77–91.
- [30] P. Drodzowski, C. Rathgeb, A. Dantcheva, N. Damer, and C. Busch, "Demographic bias in biometrics: A survey on an emerging challenge," *IEEE Transactions on Technology and Society*, vol. 1, no. 2, pp. 89–103, 2020.
- [31] J. P. Robinson, G. Livitz, Y. Henon, C. Qin, Y. Fu, and S. Timoner, "Face recognition: too bias, or not too bias?" in *IEEE Conference on Computer Vision and Pattern Recognition Workshops (CVPRW)*, 2020, pp. 0–10.
- [32] A. Das, A. Dantcheva, and F. Bremond, "Mitigating bias in gender, age and ethnicity classification: A multi-task convolution neural network approach," in *European Conference on Computer Vision Workshops (ECCVW)*, 2018, pp. 573–585.
- [33] A. Clapés, G. Anbarjafari, O. Bilici, D. Temirova, E. Avots, and S. Escalera, "From apparent to real age: Gender, age, ethnic, makeup, and expression bias analysis in real age estimation," in *IEEE Conference on Computer Vision and Pattern Recognition Workshops (CVPRW)*, 2018, pp. 2436–243609.
- [34] J. P. Robinson, C. Qin, Y. Henon, S. Timoner, and Y. Fu, "Balancing biases and preserving privacy on balanced faces in the wild," *arXiv preprint arXiv:2103.09118*, 2021.
- [35] K. Ricanek and T. Tesafaye, "Morph: a longitudinal image database of normal adult age-progression," in *International Conference on Automatic Face and Gesture Recognition (FGR)*, 2006, pp. 341–345.
- [36] B.-C. Chen, C.-S. Chen, and W. H. Hsu, "Cross-age reference coding for age-invariant face recognition and retrieval," in *Proceedings of the European Conference on Computer Vision (ECCV)*, 2014, pp. 768–783.
- [37] H. Han, C. Otto, X. Liu, and A. K. Jain, "Demographic estimation from face images: Human vs. machine performance," *IEEE Transactions on Pattern Analysis and Machine Intelligence*, vol. 37, no. 6, pp. 1148–1161, 2015.
- [38] R. Rothe, R. Timofte, and L. Van Gool, "Dex: Deep expectation of apparent age from a single image," in *Proceedings of the IEEE International Conference on Computer Vision Workshops (ICCVW)*, 2015, pp. 252–257.
- [39] H. Pan, H. Han, S. Shan, and X. Chen, "Mean-variance loss for deep age estimation from a face," in *Proceedings of the IEEE/CVF Conference on Computer Vision and Pattern Recognition (CVPR)*. IEEE Computer Society, 2018, pp. 5285–5294.
- [40] R. C. Malli, M. Aygun, and H. K. Ekenel, "Apparent age estimation using ensemble of deep learning models," *2016 IEEE Conference on Computer Vision and Pattern Recognition Workshops (CVPRW)*, pp. 714–721, Jun 2016.
- [41] W. Shen, Y. Guo, Y. Wang, K. Zhao, B. Wang, and A. Yuille, "Deep regression forests for age estimation," in *2018 IEEE/CVF Conference on Computer Vision and Pattern Recognition*, 2018, pp. 2304–2313.
- [42] T. Cootes and A. Lanitis, "The fg-net aging database," 2002, available online at <http://www-prima.inrialpes.fr/FGnet/>.
- [43] P. Phillips, H. Wechsler, J. Huang, and P. J. Rauss, "The FERET database and evaluation procedure for face-recognition algorithms," *Image and Vision Computing*, vol. 16, no. 5, pp. 295–306, 1998.
- [44] E. Agustsson, R. Timofte, S. Escalera, X. Baro, I. Guyon, and R. Rothe, "Apparent and real age estimation in still images with deep residual regressors on appa-real database," in *International Conference on Automatic Face and Gesture Recognition (FGR)*. IEEE, 2017.
- [45] Zhang, Zhifei, Song, Yang, Qi, and Hairong, "Age progression/regression by conditional adversarial autoencoder," in *Proceedings of the IEEE/CVF Conference on Computer Vision and Pattern Recognition (CVPR)*. IEEE, 2017, pp. 4352–4360.
- [46] D. Bahdanau, K. Cho, and Y. Bengio, "Neural machine translation by jointly learning to align and translate," in *Proceedings of the International Conference on Learning Representations (ICLR)*, Y. Bengio and Y. LeCun, Eds., 2015.
- [47] N. Carion, F. Massa, G. Synnaeve, N. Usunier, A. Kirillov, and S. Zagoruyko, "End-to-end object detection with transformers," in *Proceedings of the European Conference on Computer Vision (ECCV)*, A. Vedaldi, H. Bischof, T. Brox, and J.-M. Frahm, Eds. Cham: Springer International Publishing, 2020, pp. 213–229.
- [48] M. Wang, W. Deng, J. Hu, X. Tao, and Y. Huang, "Racial faces in the wild: Reducing racial bias by information maximization adaptation network," in *Proceedings of the IEEE International Conference on Computer Vision (ICCV)*, 2019, pp. 692–702.
- [49] K. S. Krishnapriya, V. Albiero, K. Vangara, M. C. King, and K. W. Bowyer, "Issues related to face recognition accuracy varying based on race and skin tone," *IEEE Transactions on Technology and Society*, vol. 1, no. 1, pp. 8–20, 2020.
- [50] A. Puc, V. Štruc, and K. Grm, "Analysis of race and gender bias in deep age estimation models," in *European Signal Processing Conference (EUSIPCO)*, 2021, pp. 830–834.
- [51] E. D. Cubuk, B. Zoph, J. Shlens, and Q. V. Le, "Randaugment: Practical automated data augmentation with a reduced search space," in *Proceedings of the IEEE/CVF Conference on Computer Vision and Pattern Recognition (CVPR)*. IEEE, 2020, pp. 3008–3017.
- [52] K. Simonyan and A. Zisserman, "Very deep convolutional networks for large-scale image recognition," in *Proceedings of the International Conference on Learning Representations (ICLR)*, Y. Bengio and Y. LeCun, Eds., 2015.
- [53] K. He, X. Zhang, S. Ren, and J. Sun, "Deep residual learning for image recognition," in *Proceedings of the IEEE/CVF Conference on Computer Vision and Pattern Recognition (CVPR)*, 2016, pp. 770–778.
- [54] J. Deng, J. Guo, N. Xue, and S. Zafeiriou, "Arcface: Additive angular margin loss for deep face recognition," in *Proceedings of the IEEE/CVF Conference on Computer Vision and Pattern Recognition (CVPR)*, 2019, pp. 4685–4694.
- [55] T. He, Z. Zhang, H. Zhang, Z. Zhang, J. Xie, and M. Li, "Bag of tricks for image classification with convolutional neural networks," in *Proceedings of the IEEE/CVF Conference on Computer Vision and Pattern Recognition (CVPR)*, 2019, pp. 558–567.
- [56] L. Liu, H. Jiang, P. He, W. Chen, X. Liu, J. Gao, and J. Han, "On the variance of the adaptive learning rate and beyond," vol. abs/1908.03265, 2020.
- [57] M. R. Zhang, J. Lucas, J. Ba, and G. E. Hinton, "Lookahead optimizer: k steps forward, 1 step back," in *Advances in Neural Information Processing Systems (NIPS)*, H. M. Wallach, H. Larochelle, A. Beygelzimer, F. d'Alché-Buc, E. B. Fox, and R. Garnett, Eds., 2019, pp. 9593–9604.
- [58] I. Loshchilov and F. Hutter, "SGDR: stochastic gradient descent with warm restarts," in *Proceedings of the International Conference on Learning Representations (ICLR)*. OpenReview.net, 2017.
- [59] H. Sun, H. Pan, H. Han, and S. Shan, "Deep conditional distribution learning for age estimation," *IEEE Transactions on Information Forensics and Security*, vol. 16, pp. 4679–4690, 2021.
- [60] S. Li and K.-T. Cheng, "Facial age estimation by deep residual decision making," *arXiv preprint arXiv:1908.10737*, 2019.
- [61] A. Krizhevsky, I. Sutskever, and G. E. Hinton, "Imagenet classification with deep convolutional neural networks," in *Advances in Neural Information Processing Systems (NIPS)*, F. Pereira, C. Burges, L. Bottou, and K. Weinberger, Eds., vol. 25. Curran Associates, Inc., 2012.